MULTI-TEMPORAL INTERFEROMETRIC POINT TARGET ANALYSIS

U. WEGMÜLLER, C. WERNER, T. STROZZI, AND A. WIESMANN

Gamma Remote Sensing AG.
Thunstrasse 130, CH-3074 Muri (BE), Switzerland
wegmuller@gamma-rs.ch, http://www.gamma-rs.ch

Abstract— Interferometric Point Target Analysis (IPTA) is a method to exploit the temporal and spatial characteristics of interferometric signatures collected from point targets to accurately map surface deformation histories, terrain heights, and relative atmospheric path delays. In this contribution the IPTA methodology is presented. Furthermore, based on examples, its applicability for stacks of ERS and JERS SAR data is validated.

1. Introduction

Natural and human induced land surface deformation is a widely observed phenomenon. Causes for deformation include tectonic, seismic, and volcanic activity, ice and rock glacier motion, slope instability, and subsidence caused by ground-water pumping, mining, hydrocarbon extraction, and natural compaction. Repeat-pass space-borne SAR interferometry is a powerful technique for the observation of land surface deformation. In areas where the method can successfully be applied, the main error source in the interferometric estimate of deformation is heterogeneity in the atmospheric path delay. Techniques for reducing this error by stacking multiple independent observations have been presented and have achieved validated accuracies in the mm/year range [1-3]. An important limitation of interferometry, though, is that the spatial coverage achieved is incomplete. Decorrelation does not permit a reliable interpretation of the interferometric phase for parts of the area. The man reasons for decorrelation are incoherent temporal change and geometric decorrelation.

Ferretti et. al. [4,5] proposed examining interferometric phases from stable, point-like reflectors and demonstrated that large numbers of such reflectors could be identified in stacks of ERS data, particularly in build-up areas. For point targets no spatial decorrelation occurs permitting interpretation of the interferometric phase of pairs with long baselines, even above the critical baseline. Obviously, the same reflector must remain stable over the time period of interest to permit analysis of the phase history.

Building upon these ideas, the main objective of our development is to achieve more complete use of the available data. Through the use of point targets, interferometric pairs with long baselines can be used. Consequently, more

observations are available permitting reduction of errors resulting from the atmospheric path delay and leading to better temporal coverage. Concerning the spatial coverage, there is the expectation that a few point targets may also be found in non-urban areas, permitting extension of the spatial coverage.

In the following sections our Interferometric Point Target Analysis (IPTA) concept is presented. Data examples are used to illustrate intermediate and final products and to confirm the validity of the concept.

2. Interferometric Point Target Analysis (IPTA) Methodology

2.1. *Data base strategy*

In the IPTA interferometric phases are only interpreted for the selected points. For efficiency and data storage reasons vector format data structures are used instead of the raster data format of conventional interferometry. This permits a drastic reduction of the required disk space. For example, only 70 MB are used to keep track of 100,000 points in a stack of 70 SLCs. Similar point data stacks in vector format are used for interferograms, unwrapped phases, topographic heights, deformation rates, residual phases associated with the atmosphere and the point coordinates. Specific programs support the conversion between vector and raster data formats.

2.2. *Interferometric phase model*

The IPTA phase model is identical to the one of conventional interferometry. The unwrapped interferometric phase ϕ_{unw} is expressed as the sum of topographic ϕ_{topo}, deformation ϕ_{def}, differential path delay (also called atmospheric phase) phase ϕ_{atm}, and phase noise ϕ_{noise} (or decorrelation) terms

$$\phi_{unw} = \phi_{topo} + \phi_{def} + \phi_{atm} + \phi_{noise} . \quad (1)$$

The sensitivity of the interferometric phase to the parameters as the terrain height and the surface deformation component along radar look vector, are found in the SAR interferometry literature, e.g. [6,7]. Also important in the context of the phase model are spatial and temporal characteristics of the different terms. For example ϕ_{atm} can be considered low-pass in the spatial domain and high-pass (random) in the temporal domain.

2.3. *Input data*

An overview on the IPTA processing sequence is given in Figure 1. The IPTA processing begins by assembling a stack of co-registered single look complex images (RSLCs), the related SLC and orbit parameters (pSLC_par), and a text file (itab) that is used to specify which pairs shall be considered in the interferometric data stacks. For a large stack of more than 10 SLCs a typical selection is that the same reference

SLC is used for all pairs. An alternative, which is particularly useful in the case of small stacks is to include all possible pairs. Furthermore, a preliminary Digital Elevation Model (DEM) is used, if available.

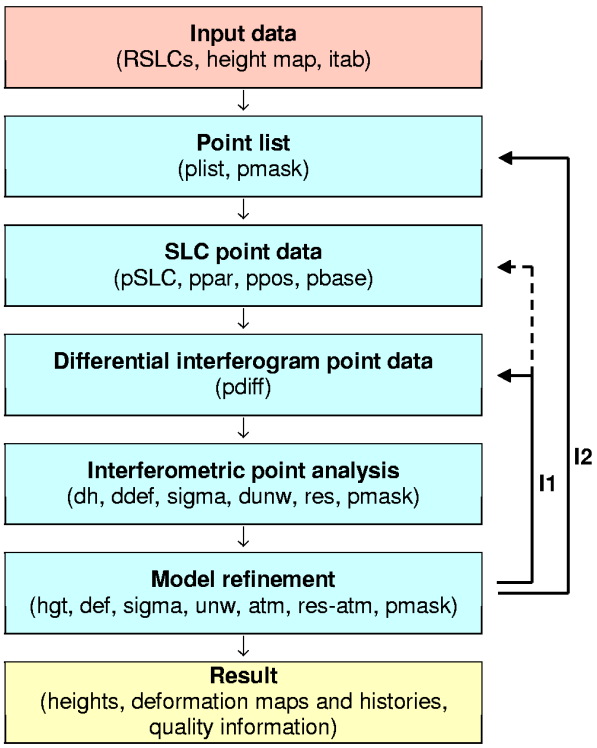

Figure 1: Interferometric point target analysis (IPTA) processing flow chart.

2.4. *Point target identification*

Based on the registered SLCs, a candidate list of point targets is determined. Point targets do not show the speckle behavior associated with distributed targets since, by definition, only a single coherent scatterer contributes to the echo. The intensity and phase are directly dependent on the point target radar cross section and position. Consequently, an initial selection of point target candidates can be performed based on the low temporal variability of the backscatter. High quality radiometric calibration and image co-registration with accurate interpolation are important technical requirements for this method. It works well for large data stacks. Alternative criteria, mainly of interest for small stacks, are high backscattering and low spectral phase diversity. At a later stage of the processing the standard deviation of the phase with respect to the interferometric phase model will become the main selection criteria.

2.5. *SLC point data and initial baseline estimation*

For the candidate points the SLC values are extracted and written to a point data stack. Initial estimates of the interferometric baselines are calculated from the available orbit state vectors.

2.6. *Differential interferograms point data*

Next, the differential interferograms are calculated. For each selected interferometric pair an unwrapped interferometric phase is simulated based on the currently available information, i.e. the initial baselines and the available DEM, and subtracted from the related interferogram. Typically, no information on deformation and atmospheric phase delay is available at an early stage of the investigation. Depending on the accuracy of the assumed model parameters and the quality of the candidate points, these differential interferograms may look smooth or very noisy. For pairs with very large baselines the accuracy requirement for the height is high, so that the related differential interferograms will look noisy (Figure 3), even when using a high resolution DEM of good quality.

2.7. *Interferometric point analysis*

In the next step the stack of differential interferograms is analyzed. This is done primarily in the temporal domain, i.e. across the layers of the stack. For the phase differences between two image points a linear dependence on the perpendicular baseline component is found, with the slope of the regression indicating the relative height correction. The phase standard deviation includes terms related to ϕ_{noise}, ϕ_{atm}, ϕ_{def}, and baseline errors. Except for ϕ_{noise}, these terms depend all on the distance between the two points. Consequently, for pairs with short spatial separation this regression analysis can be done independently of the quality of ϕ_{atm}, ϕ_{def}, and the baseline. The regression is further improved and made more robust by also considering linear phase dependence with time, equivalent to a constant deformation rate. An example of such a two-dimensional regression analysis is shown in Figure 2. The 59 points correspond to 59 differential interferometric phases. The slope in the upper plot shows that the baseline dependence is quite steep, indicating a height correction of 13.3 m. The lower plot shows a linear phase trend equivalent to a subsidence of 1.96 mm/year. One problem for the regression is that the phases in the differential interferogram are still wrapped. For large stacks performing a non-linear regression using the wrapped phase data is possible, but for small stacks, spatial phase unwrapping may be required prior to the regression step. The standard deviation of the phase from the regression is used as a quality measure, permitting to detect and reject points which are not suited for IPTA analysis.

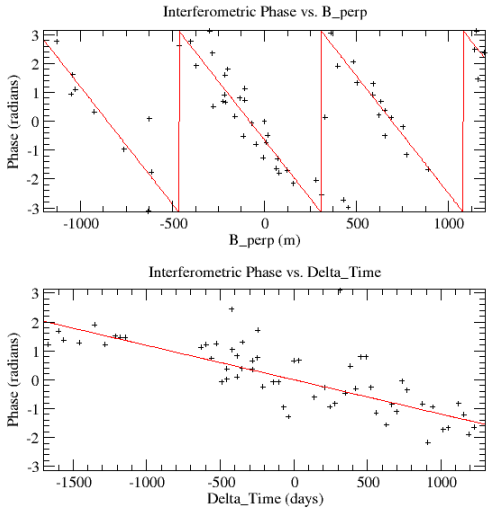

Figure. 2: Two-dimensional regression analysis of differential interferometric phase difference of two close points in a stack of 59 ERS interferograms.

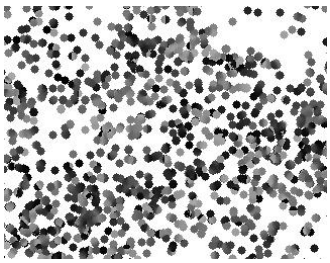

Figure 3: Differential interferometric point phases using DEM heights as reference. Area size: 6.4x5.0km^2, B_perp: 1162.47m.

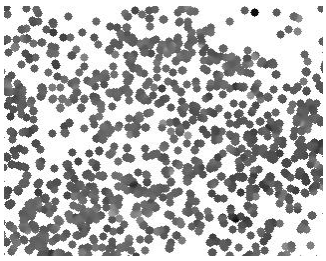

Figure 4: Differential interferometric point phases as in Figure 3 but using improved heights.

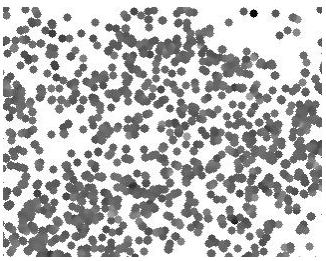

Figure 5: Differential interferometric point phases as in Figure 3 but using improved heights, baseline, and atmospheric terms.

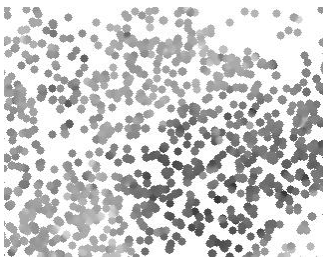

Figure 6: Linear deformation rate (linear grey scale between –5 and 2mm/year in line-of-sight). Subsiding region (dark) is associated with the Raymond Fault zone in S. Pasadena.

2.8. *Model refinement*

This regression analysis is performed for the entire point list. The results are height corrections, linear deformation rates, a quality measure, residual phases, and the unwrapped interferometric phase. These are used to improve the model. The height corrections, for example, are added to the DEM heights used in the simulation. As a validation of the successful improvement of the heights and of the interpretability of the phases of point targets in pairs with very large baselines, Figure 4 shows the differential interferogram for the same pair as in Figure 3, but uses the improved heights for the phase model.

The residual phase contains the atmospheric phase, which is related to the path delay heterogeneity at the two acquisition times of the pair, as well as non-linear deformation and error terms. Different phase terms can be discriminated based on their differing spatial and temporal dependencies. The atmospheric path delay is low-pass in the spatial dimension, but uncorrelated from pass to pass. The non-linear deformation is generally low-pass in the spatial and temporal dimension, but there may be cases where this is clearly not the case. Baseline related errors are low-pass in the spatial dimension and uncorrelated from pair to pair. Finally, the phase noise is random in both spatial and temporal dimensions.

2.9. *Iterative improvement of parameters*

An important aspect of the IPTA concept is the possibility of a step-wise, iterative improvement of different parameters. Main improvements include the consideration of a height correction, a deformation rate, a baseline refinement, atmospheric phase terms, and extension of the point list. The derivation of height corrections and constant deformation rates is done in the two-dimensional regression analysis already described.

For the baseline refinement a least-squares approach based on the unwrapped phases and the corresponding terrain heights is used. Either the original heights or the heights after the height correction can be used. The effect of linear deformation can be compensated for or the estimation can be limited to areas with no deformation.

The atmospheric phase terms are estimated from the residual phases. Discrimination of phase noise from non-linear deformation is done by considering only spectral components that are low frequency in the spatial dimension and high frequency in the temporal dimension. This is done after the refinement of the baselines, as the baseline-related errors would also fall in this spectral category. The correct separation of the atmospheric phase term, the non-linear deformation, and phase noise is not completely possible. The assumptions used in the separation may not be fully valid. To map very fast or very local deformation features the separation criteria need to be adapted accordingly. Figure 5 shows the differential interferogram for the same pair as in Figure 3, using the improved heights, the refined baselines, and the correction for the atmospheric phase.

Once the interferometric phase model closely matches the interferograms, spatial filtering of the differential interferograms to reduce signal noise becomes possible. Furthermore, it becomes possible to move from a local reference and multi-patch processing to a global reference and single patch processing.

The objective of the extension of the point list is to include as many points as possible. The evaluation of the quality of potential additional points can be done more reliably and efficiently if the improved model for the validated points is already available. This extension step also means that the first point target candidate selection can concentrate on candidates which are very likely to be point targets. Missing a fraction of the existing point targets is not severe at this stage as long as the selected points have a sufficient spatial coverage.

2.10. *Result*

At the end of the iteration the main elements of the IPTA result include linear deformation rates (see Figure 6), terrain heights, atmospheric phase terms (multiple records), precision baseline estimates (per interferogram record), deformation phase history (multiple records), and quality information. The result depends on references used, the iteration scheme, the processing parameters, and the filtering. All these need to reflect the information requirements of the specific case.

In the interpretation of the deformation rates and terrain heights it is important to remember that there may be single point effects. Many scatterers are related to buildings. Some of the scatterers are located at ground level, while others are found at roof level. Consequently, the derived heights may locally vary by up to more than 10m. Similarly, there may be local deformation effects, for example related to buildings.

3. Applicability

For much of the development a large set of 59 ERS SLCs over the densely urbanized area of Pasadena was used. This selection was motivated by the fact that the technique is expected to perform best over urban areas. The use of many scenes makes the approach more robust. Furthermore, we knew that there was deformation as well as more stable areas at this site and a digital elevation model was available. In the meantime the technique was applied to further examples, two of which are presented here. The first one is a subset of 6 ERS SLCs over Pasadena. The objective was to investigate the applicability of the technique for a much smaller stack. The second example is a stack of JERS data which was used to confirm the applicability of IPTA for this L-band sensor.

3.1. *Applicability of IPTA to small stacks*

To investigate the applicability of IPTA to small stacks, 6 consecutive repeat-pass ERS SAR acquisitions over Pasadena were selected. The main modification done to the processing was that not a single SLC was used as reference for all interferometric pairs, as for the large ERS data stack, but that each possible pair was included. For the 6 SLC this increased the number of interferograms to 15, with baselines between –300 and 900 *m* and time differences between 35 and 210 *days*. In spite of the small number of scenes included, it was indeed possible to identify point targets and interpret their phases. As shown in Figure 7 the phase unwrapping could still be resolved in the baseline – time - regression step.

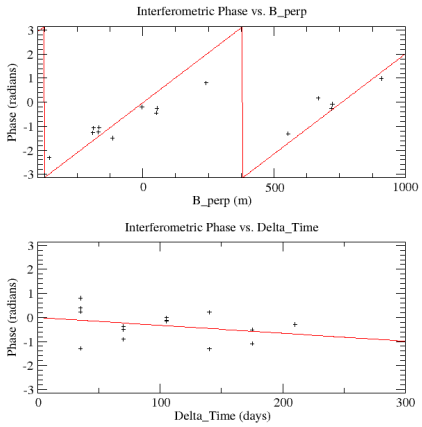

Figure. 7: Two-dimensional regression analysis of differential interferometric phase difference of two close points in a stack of 15 ERS interferograms calculated from 6 SLC.

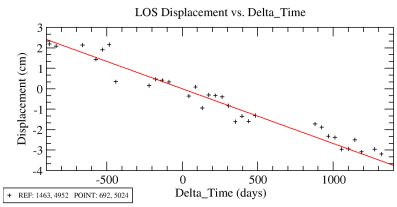

Figure 8: Deformation history of a point derived with IPTA from JERS SAR data stack. Deviation from the regression line includes non-linear deformation and noise.

3.2. *Applicability of IPTA using JERS L-band SAR*

To investigate the applicability of IPTA using JERS L-band SAR a stack of 39 repeat-pass JERS SAR acquisitions over Koga, Japan, was used. As for large ERS stacks a single JERS SLC was used as reference for all interferometric pairs. Baselines were predominantly between –4 km and +10 km acquisition dates between 1993 and 1998. The same processing sequence as applied for the large stack of ERS data was used with the only significant modification that the initial baseline estimation was improved for the interferograms with shorter baselines based on the fringe rates of the initial interferograms. This additional refinement was necessary for the higher uncertainty of the JERS orbit state vectors which may result in baseline errors of several hundred meters. The number of point targets identified was comparable to those found with ERS, i.e. > 100 km^{-2} for densely built up areas. Figure 8 shows the

deformation history for a selected point in the area. In this quite heavily urbanized area a relatively complete spatial coverage is achieved. A more detailed discussion of this example is given in [8].

4. Conclusions

The Interferometric Point Target Analysis (IPTA) methodology was presented and its applicability for stacks of repeat-pass ERS and JERS SAR data was confirmed. One experiment with a stack of 6 ERS scenes showed that the methodology is applicable even for relatively small stacks. Another experiment confirmed the applicability for JERS L-band data and indicated that similar point target densities were identified as for ERS.

The wide applicability of IPTA found in this study together with the high accuracies which can be achieved, the existing large SAR data archives, the ongoing and planned SAR missions, and the high demand for land surface deformation information are factors indicating an important role of IPTA in future multi-temporal interferometric SAR data analysis.

5. References

1. Strozzi T., U. Wegmüller, C. Werner, and A. Wiesmann, Measurement of slow uniform surface displacement with mm/year accuracy, Proc. of IGARSS'00, Honolulu, USA, 24-28 July 2000.
2. [2] Strozzi T., U. Wegmüller, L. Tosi, G. Bitelli, and V. Spreckels, Land subsidence monitoring with differential SAR interferometry, Photogrammetric Engineering and Remote Sensing, Vol. 67, No. 11, pp. 1261-1270, Nov. 2001.
3. Wegmüller U., T. Strozzi, and L. Tosi, "Differential SAR interferometry for land subsidence monitoring: methodology and examples", Proceedings of SISOLS 2000, Ravenna, Italy, 25 -29 September 2000.
4. Ferretti A., C. Pratti, and F. Rocca, Non-linear subsidence rate estimation using permanent scatterers in differential SAR interferometry, IEEE TGRS Vol 38, No.5, pp. 2202-2212, Sept. 2000.
5. Ferretti A., C. Pratti, and F. Rocca, Permanent scatterers in SAR interferometry, IEEE TGRS Vol 39, No.1, pp. 8-20, Jan. 2001.
6. Bamler, R., & Hartl, P. 1998. Synthetic aperture radar interferometry. Inverse Problems, 14, R1-R54.
7. Rosen P. et al., "Synthetic Aperture Radar Interferometry," *Proc. IEEE* vol. 88, no. 3, pp. 333- 382, 2000.
8. Werner C., U. Wegmüller, A. Wiesmann, and T. Strozzi, Interferometric Point Target Analysis with JERS-1 L-band SAR data, Procs. IGARSS'03, Toulouse, France, 21-25 July 2003.